

## Adaptive optical biocompact disk for molecular recognition

Leilei Peng<sup>a)</sup> and Manoj M. Varma

Department of Physics, Purdue University, 525 Northwestern Avenue, West Lafayette, Indiana 47907

Fred E. Regnier

Department of Chemistry, Purdue University, 560 Oval Drive, West Lafayette, Indiana 47907

David D. Nolte

Department of Physics, Purdue University, 525 Northwestern Avenue, West Lafayette, Indiana 47907

(Received 19 January 2005; accepted 25 March 2005; published online 28 April 2005)

We report the use of adaptive interferometry to detect a monolayer of protein immobilized in a periodic pattern on a spinning glass disk. A photorefractive quantum-well device acting as an adaptive beam mixer in a two-wave mixing geometry stabilizes the interferometric quadrature in the far field. Phase modulation generated by the spinning bilayer pattern in the probe beam is detected as a homodyne signal free of amplitude modulation. Binding between antibodies and immobilized antigens in a two-analyte immunoassay was tested with high specificity and without observable cross reactivity. © 2005 American Institute of Physics. [DOI: 10.1063/1.1915511]

Interferometric biosensing has the advantages of fast, tag-free, and high-sensitivity molecular detection relative to other optical biosensing techniques.<sup>1</sup> To be sensitive to phase (i.e., optical thickness), interferometry must work near the quadrature condition where the relative phase between the signal and the reference is equal to  $\pi/2$ . Most interferometric biosensing techniques use integrated interferometric sensors.<sup>2,3</sup> Free-space interferometry, on the other hand, has the advantage of multiple simultaneous spatial channels, but has suffered from perturbations and mechanical vibrations that can cause large signal drift. A free-space interferometric method with quadrature stability was recently developed. This method, called microdiffraction biocompact disk (BioCD), sets the phase of the interference by the height of gold microstructures on a spinning disk.<sup>4</sup> In this letter, we describe an adaptive solution for the phase stabilization<sup>5-7</sup> on a BioCD that does not need any microstructuring of the reaction surface. This enables multianalyte biosensing on a plain glass disk.

The adaptive optical (AO-class) BioCD uses spatially periodic patterns of biomolecules immobilized on a spinning glass disk that impart a periodic phase modulation on a probe laser beam. The probe beam is mixed with a coherent reference beam in a two-wave mixing configuration in a photorefractive quantum-well device that converts the phase modulation to an amplitude modulation. Detecting biomolecules as a spinning phase pattern has two advantages. First, biomolecules are detected by measuring signals at a high frequency, which avoids  $1/f$  noise and also allows narrowband detection based on repetitive sampling. Second, the phase signal measured by the system is the optical thickness difference between the molecular spoke pattern and a reference surface. In an assay application, the molecular spoke can be a recognition molecule like an antibody that recognizes and binds a specific molecule in a sample. The reference surface can carry an inert molecule or a molecule that is specific to a different target protein. Nonspecific protein-protein binding (called cross reactivity) will be common to both surfaces and is therefore automatically cancelled out.

The phase modulation scheme of the AO-BioCD is shown in Fig. 1. The adaptive BioCD disk (Fig. 1 bottom) is a 4 in. diameter glass disk with printed biomolecules in a 1024-wedged-spoke pattern, in which the spoke width increases linearly with the radius to maintain the pattern duty cycle. When the disk is spun at a constant 50 Hz speed, the protein pattern is transferred onto the 30  $\mu\text{m}$  diameter probe beam as a time-domain phase modulation at 51 kHz. The spinning BioCD thus acts as a phase modulator with a modulation depth that is linear in the optical thickness relief of the biomolecule pattern. Detection is performed on circular tracks with radii that are selected by moving the spinner with a computer-controlled linear stage. To provide a reference signal for lock-in detection, the disk has 1-mm-wide gold-patterned synchronization tracks on the outer rim providing from 1st to 16th harmonic signals of the rotation frequency

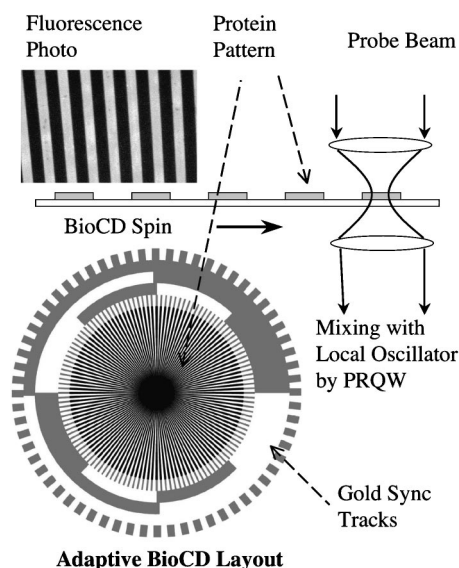


FIG. 1. The AO-BioCD disk and probe geometry that converts a periodic pattern of printed protein on a spinning disk into a high-frequency phase modulation. The figure shows the adaptive BioCD layout (bottom), the probing scheme (top-right), and fluorescence photo of the protein pattern (top-left).

<sup>a)</sup>Electronic mail: pengl@physics.purdue.edu

(only three tracks are shown in the layout), plus a 1024 element track as a carrier frequency monitor.

The phase-modulated probe beam is sent into a photorefractive quantum well (PRQW) device<sup>8</sup> and mixed with a local oscillator beam by two-wave mixing,<sup>9</sup> which can self-compensate environmental and mechanical disturbances to maintain the quadrature condition with a compensation rate higher than a kHz.<sup>10</sup> Phase modulation in the probe beam at frequencies higher than the compensation rate of the PRQW device is read out by a photodetector as amplitude modulation caused by interference between the reference beam and the first-order diffraction of the signal beam. The phase difference between the two fields is tuned to the quadrature condition<sup>9</sup> by selecting the operating wavelength (near 830 nm) at which homodyne signals depend linearly on phase modulation. Homodyne detection in photorefractive materials has been applied in ultrasound detection with subpicometer sensitivity to optical path change,<sup>11,12</sup> which is much less than a monolayer of biological macromolecules such as antibodies (5–8 nm).

In the probe beam, the amplitude noise caused by diffraction from the spatial index variations in the disk is typically much stronger than the molecular signal. Extracting small phase modulation in the presence of large amplitude modulation is difficult for conventional interferometry, in which the probe and the local oscillator are directly mixed and the amplitude noise in the probe beam dominates. However, the adaptive interferometer has separate output ports for the probe beam and local oscillator, which makes it possible to detect the molecular signal in the local oscillator that is free of amplitude modulation. Under the condition of quadrature, the transmitted local oscillator is influenced only by the molecular signal and by the phase noise in the probe beam.

The system uses a tunable external cavity diode laser (EOSI 2010), whose wavelength is tuned to quadrature near 830 nm. After mixing the probe beam and the local oscillator in the PRQW device, homodyne signals are read out by an amplified avalanche photodiode (Hamamatsu C5460) centered on the local oscillator beam and measured by either a spectrum analyzer or a lock-in amplifier. To validate the system, a 5-MHz-resonant phase modulator (Newfocus 4001) is placed in the probe beam before the BioCD disk, and a homodyne signal is measured with known phase-modulation amplitudes. The frequency response of the PRQW device was verified to be the same between 50 kHz and 5 MHz allowing phase modulations from BioCD disks are calibrated by comparing their homodyne signals with the phase-modulator signal.

Figure 2(a) plots the 3-kHz-bandwidth homodyne spectrum from a BioCD disk printed with Bovine serum albumin (BSA) by an “ink” gel stamping method in which a polyacrylamide patterned gel stamp containing BSA is brought into contact with the BioCD disk, whose surface has been activated with chlorodimethyloctadecylsilane. Protein is transferred to the disk surface by physical adsorption.<sup>13</sup> Fluorescein conjugated BSA (Sigma) was used to verify printing, and the fluorescence photo [Fig. 1 top] shows a uniform intensity. The spectrum, combined with the phase-modulator calibration [Fig. 2(b)] determined that the BSA pattern has an optic thickness  $(n-1)d=0.6$  nm. The physical thickness of the pattern was also measured using atomic force microscope, shown as the insert in Fig. 2(a) as a height gray-scale map of a  $10 \times 10 \mu\text{m}$  scan on the edge of one spoke. The

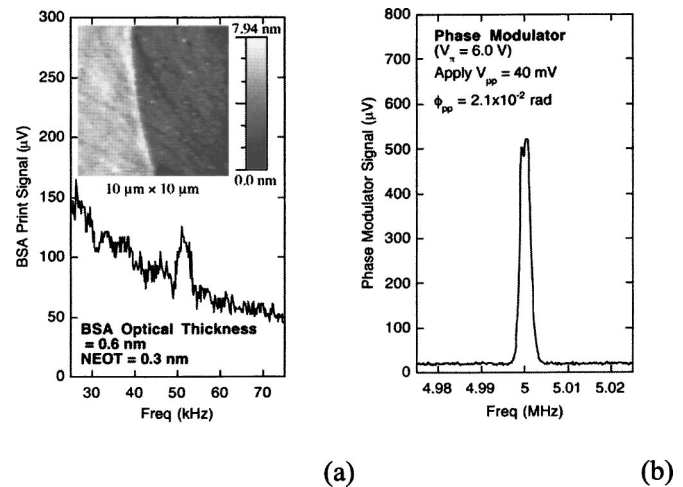


FIG. 2. The AO-BioCD calibration. (a) The homodyne signal spectrum of printed BSA. Insert: the atomic force microscope scan of the edge of one BSA spoke. (b) The homodyne signal spectrum of the phase modulator, driven by a 5 MHz ac voltage with  $V_{pp}=40$  mV, which generates a phase modulation of  $\phi_{pp}=2.1 \times 10^{-2}$  rad for an equivalent optical thickness of 2.8 nm.

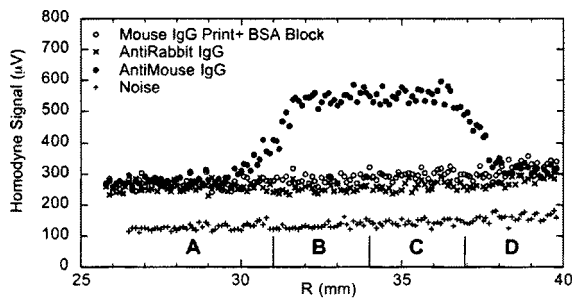
scan measured the BSA region  $2.5 \pm 0.7$  nm higher than the glass region, which verified that the BSA was printed as a protein monolayer and also confirmed a refractive index of  $1.2 \pm 0.1$  for BSA.

The signal-to-noise ratio of the system is determined by the noise equivalent optical thickness (NEOT), defined through the expression

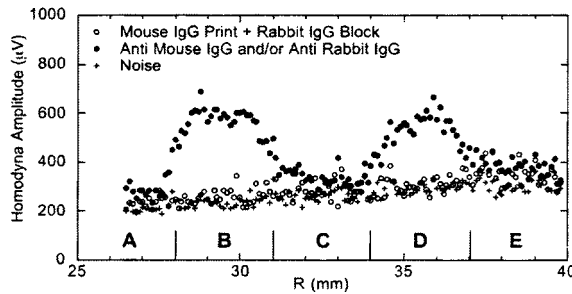
$$\frac{S}{N} = \frac{(\delta P'_L)^2}{N_L^2 + N_P^2} = \left( \frac{\delta d}{\text{NEOT}} \right)^2, \quad (1)$$

where  $N_L$  and  $N_P$  are noise amplitudes contributed by the local oscillator and the phase noise from the disk, respectively. At the 51-kHz-modulation frequency,  $N_P$  dominates, which gives a NEOT equal to 0.3 nm. Much higher sensitivity can be achieved by narrowing the detection bandwidth with lock-in detection, because lock-in noise measurements show that NEOT caused by the disk phase noise decreases linearly to the detection bandwidth. However, the current system is limited to a detection bandwidth of approximately 3 kHz due to mechanical factors. Future technical improvements should allow narrower detection bandwidths and more sensitive thickness measurements.

We have implemented the AO-BioCD as an immunoassay seeking antigen-antibody molecular recognition. First, a mouse IgG 1024-spoke pattern was printed on the disk surface, after which the free surfaces (unprinted areas) were saturated by BSA. The disk was divided into four annular tracks (A–D) for sample incubation. Nonspecific binding was tested first by incubating track C with 200  $\mu\text{g}/\text{ml}$  anti-rabbit IgG antibody solution for 30 min. Specific binding was tested after applying 200  $\mu\text{g}/\text{ml}$  anti-mouse IgG solution to Tracks B and C. Homodyne signal amplitudes, which were scanned across the disk in 0.1 mm radius steps, recorded the optical thickness difference between the mouse IgG areas and the BSA-saturated areas. Figure 3(a) shows that no signal change occurred after the incubation with (nonspecific) anti-rabbit IgG. Subsequently, after being exposed to (specific) anti-mouse IgG, Tracks B and C showed approximately equal signal increases. This result demonstrates that the tech-



(a)



(b)

FIG. 3. The AO-BioCD Immunoassay results. (a) Single-analyte experiment detecting specific binding between mouse IgG and anti-mouse IgG. Tracks B and C are incubated with specific antibody, showing positive detection. (b) Two-analyte experiment detecting specific bindings between mouse IgG (rabbit IgG) and anti-mouse IgG (anti-rabbit IgG). Tracks B and C were incubated with rabbit, and C and D were incubated with mouse antibody. The overlapping detection in Track C cancels out.

nique recognizes target antibody, and also shows that the prior exposure to non-specific reagents does not affect the molecular recognition.

We then performed a two-analyte assay. Mouse IgG was again printed on the disk in a 50% duty-cycle 1024 spoke pattern, but this time rabbit IgG antigen was used as the free-surface saturating reagent, instead of the BSA. This generated a pattern of alternating spokes of mouse and rabbit antigen. Because both proteins had almost the same optical thickness, the disk homodyne signal amplitudes were the same as the noise level, as shown in Fig. 3(b). In the incubation process, Tracks B and C were first exposed to anti-

rabbit IgG antibody, and Tracks C and D were subsequently exposed to anti-mouse IgG. Antibody incubation generated homodyne signal peaks on both Tracks B and D, corresponding to positive detections of anti-rabbit IgG and anti-mouse IgG, respectively. On Track C, a double positive response to both antibodies canceled out the homodyne signal, as shown in Fig. 3(b). This experiment demonstrates that mouse IgG to anti-mouse IgG binding has the same high affinity as the rabbit IgG to anti-rabbit pair.

In conclusion, we have demonstrated the first adaptive interferometric BioCD for molecular recognition. The sensitivity for transmission through the glass disk was determined to be 0.3 nm, with significant future improvements possible by shifting to a reflection geometry that will not be sensitive to density fluctuations in the glass. No observable cross reactivity was observed between two-analyte binding. With future developments improving sensitivity, increasing track density and increasing the number of analytes, this technique opens the door to high-speed high-throughput biomolecular screening.

This work was supported by the National Science Foundation under Grant No. ECS-0200424.

- <sup>1</sup>F. S. Ligler and C. A. R. Taitt, *Optical Biosensors: Present and Future*, 1st ed. (Elsevier Science, Amsterdam, Netherland, 2002).
- <sup>2</sup>A. Brandenburg, R. Krauter, C. Künzel, M. Stefan, and H. Schulte, *Appl. Opt.* **39**, 6396 (2000).
- <sup>3</sup>B. Drapp, J. Piehler, A. Brecht, G. Gauglitz, B. J. Luff, J. S. Wilkinson, and J. Ingenhoff, *Sens. Actuators B* **38**, 277 (1997).
- <sup>4</sup>M. M. Varma, D. D. Nolte, H. D. Inerowicz, and F. E. Regnier, *Opt. Lett.* **29**, 950 (2004).
- <sup>5</sup>I. Rossomakhin and S. I. Stepanov, *Opt. Commun.* **86**, 199 (1991).
- <sup>6</sup>R. K. Ing and J.-P. Monchalain, *Appl. Phys. Lett.* **59**, 3233 (1991).
- <sup>7</sup>F. M. Davidson and L. Boutsikaris, *Opt. Eng. (Bellingham)* **29**, 369 (1990).
- <sup>8</sup>Q. Wang, R. M. Brubaker, D. D. Nolte, and M. R. Melloch, *J. Opt. Soc. Am. B* **9**, 1626 (1992).
- <sup>9</sup>D. D. Nolte, T. Cubel, L. J. Pyrak-Nolte, and M. R. Melloch, *J. Opt. Soc. Am. B* **18**, 195 (2001).
- <sup>10</sup>S. Balasubramanian, I. Lahiri, Y. Ding, M. R. Melloch, and D. D. Nolte, *Appl. Phys. B: Lasers Opt.* **68**, 863 (1999).
- <sup>11</sup>I. Lahiri, L. J. Pyrak-Nolte, D. D. Nolte, M. R. Melloch, R. A. Kruger, G. D. Bacher, and M. B. Klein, *Appl. Phys. Lett.* **73**, 1041 (1998).
- <sup>12</sup>P. Delaye, A. Blouin, D. Drolet, L.-A. Montmorillon, G. Roosen, and J.-P. Monchalain, *J. Opt. Soc. Am. B* **14**, 1723 (1997).
- <sup>13</sup>J. Duchet, J. F. Gérard, J. P. Chapel, and B. Chabert, *J. Adhes. Sci. Technol.* **14**, 691 (2000).